# An EOF Analysis of the Vertical–Time Delay Structure of the Quasi-Biennial Oscillation

KLAUS FRAEDRICH, STEVEN PAWSON, AND RISHENG WANG

*Institut für Meteorologie, Freie Universität Berlin, Berlin, Federal Republic of Germany*

(Manuscript received 24 February 1992, in final form 14 July 1992)

ABSTRACT

Empirical orthogonal function analyses of the time–height series of monthly mean zonal wind in the stratosphere have been performed. Conventional EOF analysis on the time series reveals that the quasi-biennial oscillation (QBO) of the zonal wind is a quasi-regular oscillation with a period near 28 months, but the noisy structure of the first two EOFs, representing 57.18% and 36.24% of the variance of the time series, leads to little new insight concerning the dynamics of the QBO. A second type of analysis is performed by applying windows to the data and calculating the EOFs of the time development of the spatial structure. By using a window of around one-half of the period of the dominant oscillation, the EOF analysis reveals that the QBO is essentially a linear feature, with successive wind regimes propagating smoothly downwards with a spectral peak near 28 months; this oscillation has a very smooth phase portrait and cross-correlation analysis of the first two EOFs reveals that it is a quasi-linear feature with good predictability. Delays in the downward propagation of the easterly phase of the QBO are shown to be nonlinear, unpredictable features, represented by higher-order EOFs.

## 1. Observations and theory of the QBO

The quasi-biennial oscillation (QBO) of the zonal wind dominates the dynamics of the tropical stratosphere between 70 and 10 hPa. First observed by Reed et al. (1961) and Veryard and Ebdon (1961), the structure of the oscillation has continued to be a topic of discussion. More recent observations of the QBO were presented by Naujokat (1986) (see also Naujokat et al. 1991), who examined the time–height structure, and by Hamilton (1984) and Dunkerton and Delisi (1985), who also examined the latitudinal structure.

The QBO is characterized by the successive downward propagation of easterly and westerly wind regimes. While the westerly wind onset generally occurs quite smoothly, with a descent rate of $\partial\bar{u}/\partial t = 1.2$ m s$^{-1}$ mo$^{-1}$, the onset of easterlies is slower and often delayed; Dunkerton (1990) argued that at 50 hPa, the onset of QBO easterlies seldom occurs in northern winter. Naujokat (1986) showed that the mean QBO period between 1953 and 1985 at 30 hPa was 27.7 months (the mean period including data up to April 1991 is 28.1 months); above 30 hPa easterlies have a longer duration than westerlies, while at higher pressures this is reversed. In the mean, the easterly wind maxima of more than 30 m s$^{-1}$ near 20 hPa are stronger than the westerly maxima of 15 m s$^{-1}$.

The generally accepted theory of the QBO is that of Holton and Lindzen (1972, hereafter HL), a modified version of that by Lindzen and Holton (1968) following the theoretical advances of Lindzen (1971) concerning the thermal dissipation of tropical waves. The momentum sources for the zonal-mean acceleration arise from such dissipation of Kelvin or mixed Rossby–gravity (hereafter MRG) waves immediately below their critical levels, where their vertical group velocity is slow enough for the dissipation to become effective. A deficiency of this model is that the asymmetry of the oscillation is reversed from that observed: the easterly winds propagate more rapidly downwards than the westerlies. Two-dimensional (latitude–height) model studies by Plumb and Bell (1982) and Dunkerton (1985) have shown that the induced meridional circulation acts to restore the correct asymmetry in onset of the regimes.

Furthermore, the observed QBO often exhibits a delay in the onset of the easterly winds when their downward propagation is interrupted, often for several months, between 30 and 50 hPa. Additional forcing mechanisms, or extensions to the HL model, are required to account for this. Dunkerton (1990) argued that the easterly wind onset at 50 hPa preferentially occurs in Northern Hemisphere spring and summer, which suggests that some annual modulation of the easterly forcing, with a minimum in Northern Hemisphere fall and winter, could be responsible for this delay in onset. Maruyama (1991) found an annual variability in the observed MRG waves over Singapore, consistent with this concept of "preferred time of onset" of the easterlies. Andrews and McIntyre (1976) suggested that planetary waves could propagate from the

*Corresponding author address:* Steven Pawson, Institut für Meteorologie, Freie Universität Berlin, Carl-Heinrich-Becker Weg 6-8, Berlin 41, FRG, W-10.

winter stratosphere and contribute to the easterly forcing.

The objective of this paper is to analyze the observed zonal-mean zonal wind over Singapore in a manner that isolates its evolution in a dynamically meaningful manner, in the hope that some physical explanation of the QBO can be obtained. The irregular period and variable vertical structure of the QBO make conventional harmonic analysis inadequate. Therefore, an empirical orthogonal function (EOF) analysis, in which no a priori assumptions about structure are made, is applied. We present an EOF analysis of the wind data in section 3; although this analysis depicts the vertical structure of the QBO, it is inadequate for interpretation of the dynamical development. Our main results are in section 4, where an EOF analysis of the temporal evolution of the vertical structure is presented; this facilitates the interpretation of the dynamical development of the QBO. The final section summarizes our results and discusses our interpretation of the QBO; we suggest that the analysis has clarified the interpretation of several important features of the QBO, and address some further problems to be tackled. First the data are summarized.

## 2. Data used

Zonal-mean zonal wind data from Naujokat (1986) and Naujokat et al. (1991) are used in this study; they are available at seven levels (70, 50, 40, 30, 20, 15, and 10 hPa) between January 1953 and April 1991. Since the upper-level data are missing from the first three years, the time series has been analyzed from 1956 onward. Monthly mean values were used in this study; on the occasions when there were no observations throughout the month, the data were linearly interpolated; in some months, few observations were available, but these have nevertheless been included. In the following, the state vector of the wind for any month, $n$, is denoted by $\mathbf{u}^n = [u^n(k)]$, $k = 1, 2, \cdots, K = 7$ (where the level $k$ increases upwards).

The data source has changed twice over the observation period. From January 1953 until August 1967, the data are from Canton Island (2°46'S, 171°43'W); Gan, Maldive Island, (0°41'S, 73°09'E) data are used from September 1967 until December 1975; and data for January 1976–April 1991 are from Singapore (1°22'N, 101°55'E). The analysis in this paper assumes that no artificial trends occur in the data due to these changes.

TABLE 1. The contribution of the seven EOFs to the total variance of $u^n$.

| EOF | Percent of variance | Running total |
|---|---|---|
| 1 | 57.18 | 57.18 |
| 2 | 36.24 | 93.42 |
| 3 | 2.84 | 96.25 |
| 4 | 2.09 | 98.35 |
| 5 | 0.82 | 99.16 |
| 6 | 0.55 | 99.71 |
| 7 | 0.29 | 100.00 |

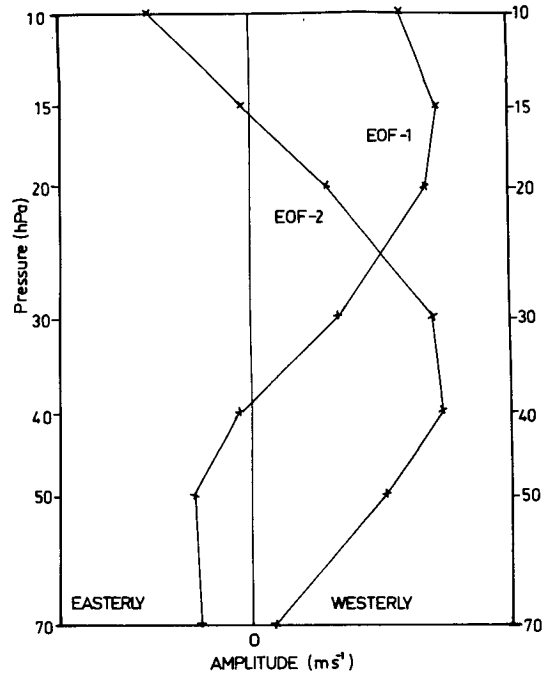


FIG. 1. The vertical structure of EOFs 1 and 2 that represent the QBO (positive values represent westerlies and the amplitude is arbitrary).

## 3. Stationary EOF patterns

Conventional EOF analysis is applied to the vertical structure of $\mathbf{u}^n$ in this section. Similar analyses have recently been presented by Xu (1992), who used principal oscillation patterns (POPS) to examine relationships between the QBO and ENSO, and by Wallace et al. (1993), who analyzed the phase propagation of the QBO using EOFs; the emphasis of these papers was different from this work. The seven EOFs are the eigenvectors of the covariance of the time series of $\mathbf{u}^n$, the amplitude, $a_j(t)$ of the $j$th EOF representing its time development. The eigenvalues are defined as the variance of $a_j(t)$, and the rank of each eigenvector is ordered by the magnitude of the eigenvalue. The eigenvectors are thus ordered by the magnitude of their eigenvalues, so that EOF 1 represents the largest part of the total variance, EOF 2 the second largest part, and so on. In general, one hopes that a large part of the variance can be represented by a small subset of the total number of eigenvectors, which then represent the dominant signals in the data series.

The analysis reveals that EOF 1 contributes 57.18% of the variance and EOF 2, 36.24% with the remaining five accounting for only 6.58% (Table 1). The vertical structure of EOFs 1 and 2 (Fig. 1) shows the two states

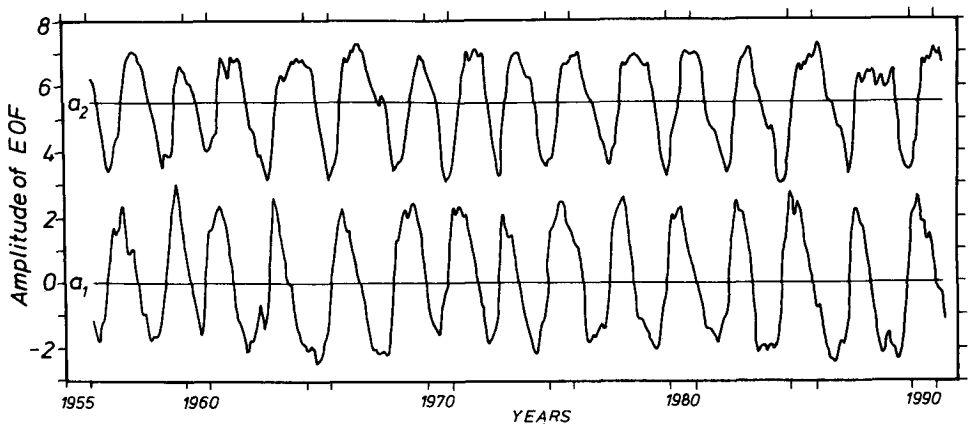


FIG. 2. Time series of $a_1$ and $a_2$.

of westerly wind overlying easterlies (EOF 1) and westerly winds dominating in the middle stratosphere (EOF 2); Fig. 2 reveals that $a_1(t)$ and $a_2(t)$ are generally around a quarter wavelength out of phase, so that their amplitude maxima are two distinct phases of the QBO. Power spectrum analysis of $a_1$ and $a_2$ shows a dominant peak at 28.4 months (representing the QBO) but also signals at shorter time scales, particularly a semiannual oscillation.

Despite the quasi regularity of $a_1$ and $a_2$, there are small-scale variations imposed upon the dominant oscillation. In particular, $a_2$ tends to flatten out near its maximum; this is the manifestation in the EOFs of the delayed onset of easterly winds between 30 and 50 hPa. This shows up clearly in the phase portrait of EOFs 1 and 2 (Fig. 3), which has a flat-topped appearance because $a_1$ takes a range of values, while $a_2$ fluctuates near its maximum. A perfectly sinusoidal wave progression would have a circular phase portrait, the radius of which expresses its amplitude. The irregular structure of Fig. 3 illustrates the small-scale irregularities in the EOF analysis more clearly than Fig. 2, the jagged structure of the phase portrait being indicative of the short-period variations in the amplitudes of the first two EOFs.

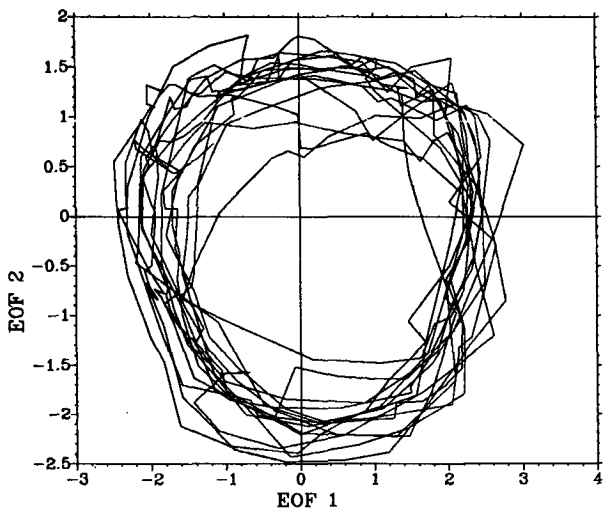


FIG. 3. The phase portrait of EOFs 1 and 2, that is, $a_1$ versus $a_2$.

The higher-order eigenvalues account for little of the variance, so they are not discussed in detail; EOFs 3 and 4 have minima at the QBO period and maxima on the semiannual and longer periods.

In summary, it seems that little new dynamical information about the QBO can be obtained through such an EOF analysis. The coefficients may, however, be useful for certain applications—for instance, sorting the atmosphere into different phases of the QBO for short-period dynamical studies when the evolution of the tropical structure may be less important than the actual structure.

## 4. EOF analysis of the height–time delay structure

The EOF analysis used in section 3 isolates the spatial structure of the QBO in the time series of winds. This does not, however, facilitate interpretation of the dynamical evolution of the QBO (or, in general, of other quasi-regular oscillations). Because one may expect the spatial evolution of the atmosphere to have some coherency in time (that is, the state of the atmosphere at one moment depends upon its history), it seems reasonable to look for coherent patterns in the time evolution of the spatial structure. Such a technique is described and applied in this section.

The method is related to the singular spectrum analysis (SSA) described by Broomhead and King (1986), Fraedrich (1986), and Vautard and Ghil (1989), which has been applied to the analysis of ENSO time series by Rasmusson et al. (1990). However, SSA does not include spatial structure. Weare and Nasstrom (1982) applied time-delayed EOF analysis to the monthly mean 300-hPa relative vorticity field with a 3-month

time delay and Pacific SST data at times $t$, $t + 3$, and $t + 6$ months. In general, the method is applicable to the time development of the three-dimensional spatial structure. Here (section 4b) it is used to describe the evolution of $\mathbf{u}^n$ with a considerably longer window than was used by Weare and Nasstrom.

### a. *Extended EOF analysis with time delay*

#### 1) TIME DELAY COORDINATES

The time delay coordinate was used by Fraedrich and Lutz (1987) to define a modified Hovmöller diagram, with coordinates of longitude and time delay, which emphasizes propagating features of dynamical significance. A similar method is used here for the vertical time structure. By sliding a window of length $W$ along the time series of $\mathbf{u}^n$, a dynamical state vector, $\mathbf{U}^n$, can be defined for each $n$. This vector has dimension $K \times W$, the columns being the vectors $\mathbf{u}^{n-W+1}$, $\mathbf{u}^{n-W+2}, \ldots, \mathbf{u}^n$. This is shown schematically in Fig. 4, where the stippled area represents $\mathbf{U}^n$. For a time series of length $T$, a total of $T - W$ vectors $\mathbf{U}^n$ can be determined; the crossed region at the beginning of the figure represents the times at which $\mathbf{U}$ is not defined.

#### 2) EOF ANALYSIS

Having defined $\mathbf{U}^n$, it is a relatively trivial matter to apply an EOF analysis to it in the standard manner. That is, the time mean of $\mathbf{U}^n$ is determined and removed, and the eigenvectors of the covariance of this time-dependent part of $\mathbf{U}^n$ represent the EOFs. The EOFs have dimension $K \times W$ and describe the dominant patterns of the vertical–time delay structure of the time series of $\mathbf{u}^n$. The amplitude (or principle component, PC) $A_j(t)$ of the $j$th eigenvector is determined at each time. As before, the eigenvalues are ordered according to their rank.

#### 3) IDENTIFICATION OF DYNAMICAL STRUCTURES

The different dynamical features in the time series are isolated by the EOF analysis. Propagating waves in the space–time delay coordinates are represented by a pair of EOFs, with similar eigenvalues and whose patterns are shifted by a quarter of a wavelength (the obvious example being a propagating sinusoidal wave whose EOFs are sine and cosine waves with equal amplitudes). The period and the wavelength are simply the distance between successive maxima on, respectively, the time delay or space axes of the eigenvalue diagram. For a perfect wavelike motion, the phase portrait of the $A_j(t)$ of the EOF pair describes a circle whose radius is proportional to the wave amplitude. In the manner of Fraedrich and Lutz (1987), the phase and group velocities of such waves can be deduced from the spatial–temporal patterns of the EOFs; the phase velocity is defined by the slope of the anomaly centers on the space–time delay diagram and the group velocity is the slope of the line between successive anomalies of opposite sign.

Nonwavelike motions in the system are represented by "single" EOFs—that is, eigenvectors that do not have a phase-shifted counterpart and do not necessarily show a tilting phase structure. Such EOFs can be used to identify discontinuities or standing waves in the time series.

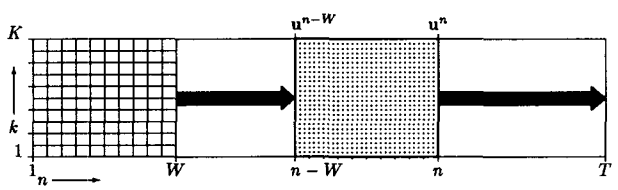


FIG. 4. Schematic representation of the definition of the dynamical state vectors as applied to the time series of the vector $\mathbf{u}^n$, representing the zonal-mean zonal wind at each level $k = 1, 2, \cdots, K$. The horizontal axis shows the time, increasing from $n = 1$ to $n = T$, with the window of length $W$, which slides along the time series from $t = W$ to $t = T$, defining a state vector (stippled area) $\mathbf{U}_n$, of dimension $K \times W$, at each of these times. Thus, $\mathbf{U}_n$ is defined at $(T - W)$ times, the checkered area, or the first $W$ times, having no dynamical state vector, and $\mathbf{U}_n = [\mathbf{u}_{n-W}, \mathbf{u}_{n-W+1}, \cdots, \mathbf{u}_n]$.

TABLE 2. The contribution of the first ten EOFs in the height–time delay analysis to the total variance of $u^n$.

| | $W = 15$ | | $W = 40$ | |
|---|---|---|---|---|
| EOF | Percent of variance | Running total | Percent of variance | Running total |
| 1 | 42.47 | 42.47 | 37.47 | 37.47 |
| 2 | 41.27 | 83.74 | 36.60 | 74.07 |
| 3 | 3.79 | 87.53 | 4.31 | 78.38 |
| 4 | 2.24 | 89.78 | 4.02 | 82.40 |
| 5 | 1.23 | 91.01 | 2.60 | 84.99 |
| 6 | 1.10 | 92.10 | 1.99 | 86.98 |
| 7 | 0.97 | 93.08 | 1.60 | 88.58 |
| 8 | 0.74 | 93.81 | 0.88 | 89.46 |
| 9 | 0.54 | 94.35 | 0.73 | 90.19 |
| 10 | 0.52 | 94.87 | 0.60 | 90.79 |

Nonwavelike motions in the system are represented by "single" EOFs—that is, eigenvectors that do not have a phase-shifted counterpart and do not necessarily show a tilting phase structure. Such EOFs can be used to identify discontinuities or standing waves in the time series.

#### 4) RECONSTRUCTION OF THE TIME SERIES

From knowledge of the amplitudes of the EOFs and their spatial–time delay structure, the original time series can be reconstructed. In the case of EOF analysis with time delay, each reconstruction generates a portion of data of length $W$. In the results presented below, the last month of each reconstruction is shown.

### b. *The height–time delay structure of the QBO*

#### 1) CHOICE OF WINDOW

The application of a window to a dataset leads to some smoothing. Here we show the significance of this to the results of this study. Eigenvalues of the dominant EOFs are shown in Table 2 for $W = 15$ and $W = 40$.

In both cases, the first two eigenvectors represent a large fraction of the total variance: 42.47% and 41.27% for $W = 15$ and 37.47% and 36.60% for $W = 40$.

Reconstruction of the time series using the mean (which shows easterlies overlying westerlies in both cases, consistent with the fact that the easterlies are strongest at high levels but westerlies at low levels) plus the first two EOFs shows an important difference between the two choices of window. Between January 1968 and December 1979, when the QBO was quite regular, the reconstruction with $W = 15$ (Fig. 5b) shows quite good agreement with the original time series (Fig. 5a) in that the westerlies propagate downwards at a constant rate between 10 and 70 hPa but the easterlies propagate downwards more rapidly above 30 hPa than below this level. That is, easterlies dominate the upper levels and westerlies the lower levels, as in the original data. In contrast, in the reconstruction with $W = 40$ (Fig. 5c), the two phases of the QBO propagate downwards at the same rate and the easterlies have a longer duration than the westerlies at all levels. The reason for this is that by applying the window longer than the period of the QBO, both phases are smoothed together; EOFs 1 and 2 have identical structures shifted by a quarter wavelength and a very regular phase progression. The asymmetry in the onset of the two phases with $W = 40$ is represented in EOFs 3 and 4, which thus include an important part of the QBO with the longer window. Note that EOFs 1 and 2 with $W = 15$ represent 83.74% of the total variance, whereas EOFs 1–4 are needed to account for 82.4% of the variance with $W = 40$ (Table 2) because of the smoothing by the longer window.

The dynamics of the QBO are represented more accurately with $W = 15$, close to half of the period so that the two phases are not smoothed together, than when the window exceeds the period of the oscillation. These EOFs are now discussed in more detail.

### 2) THE DOMINANT QBO SIGNAL WITH A 15-MONTH WINDOW

EOFs 1 and 2 (Figs. 6a,b) have very similar vertical–time delay structures, the maximum propagating downward with increasing time, with EOF 2 phase shifted by a quarter of a wavelength relative to EOF 1. Their amplitudes (Fig. 6c) are consistently a quarter wavelength out of phase. Together they thus represent the downward-propagating oscillation with asymmetrical onset of easterly and westerly winds, as already discussed (Fig. 5b). Power spectrum analysis of both of the EOFs shows a sharp peak at 28.4 months.

The phase portrait of this EOF pair (Fig. 7) has an almost constant radius, implying an almost constant amplitude of the oscillation; apart from one instance when the radius was reduced by around 40% in the lower left-hand quadrant, the amplitude remains within 20% of its mean value. The exceptional year can be identified as 1962–63 (Fig. 6c) when the amplitude of EOF 2 did not reach its normal minimum; whether or not this is related to the Mt. Agung eruption is not clear. The signal obtained here is thus much cleaner

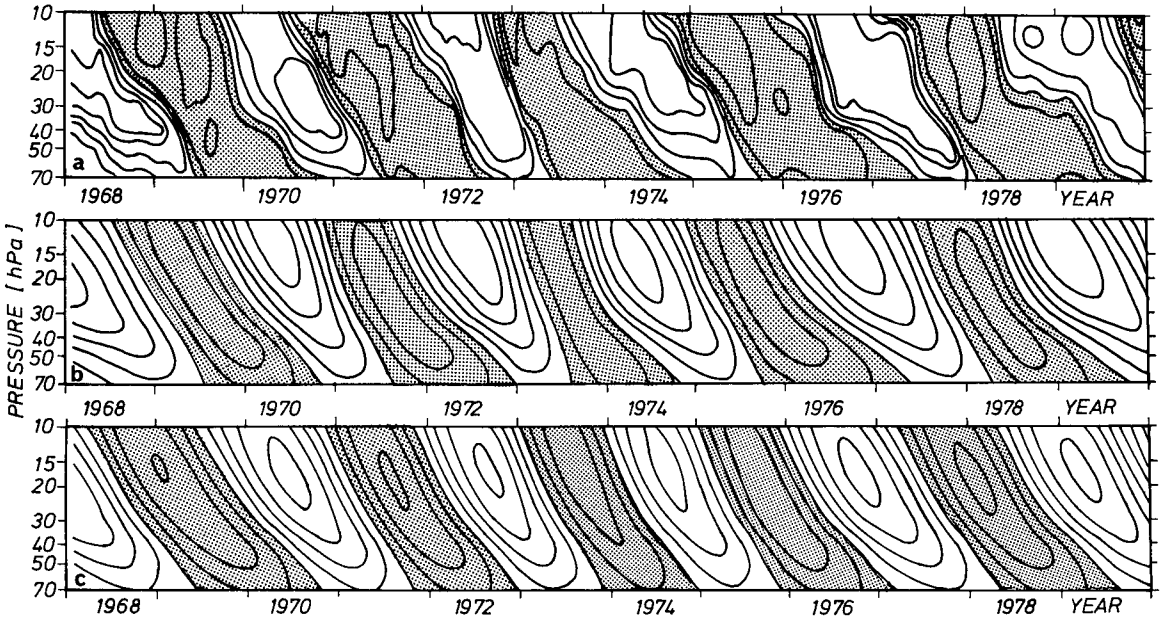


FIG. 5. (a) Time series of zonal wind data from January 1968 to December 1979. (b) Reconstruction of this time series using EOFs 1 and 2 with $W = 15$. (c) Reconstruction of this time series using EOFs 1 and 2 with $W = 40$. The lightly shaded regions represent easterly winds.

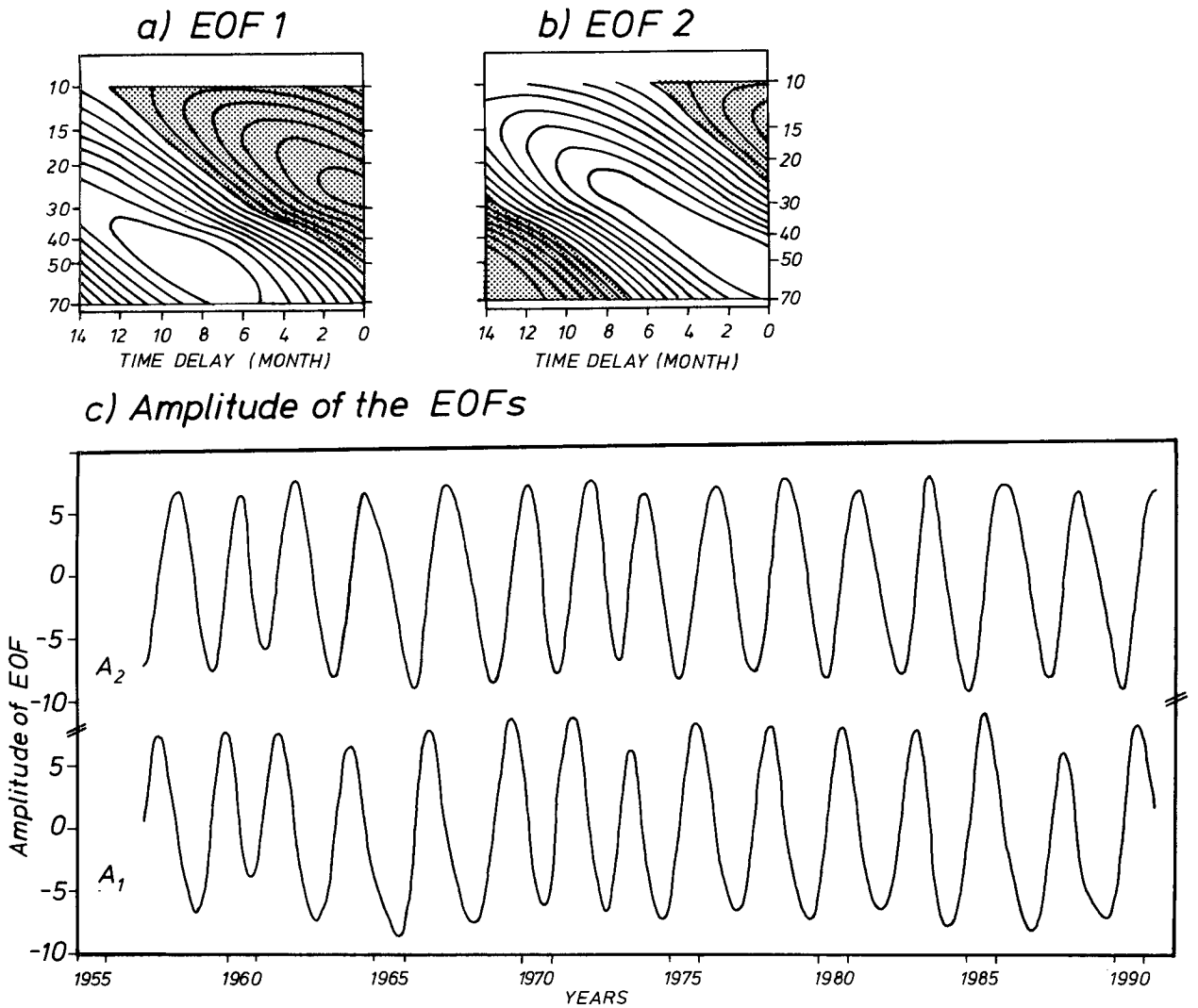


FIG. 6. EOFs 1 and 2, which represent the QBO in the vertical–time delay analysis. (a). (b) The vertical–time delay structure of EOFs 1 and 2 (lightly shaded areas are negative and the contours are arbitrary). (c) Time series of $A_1$ and $A_2$.

than that in the EOF analysis of the spatial structure, where the phase portrait of the first two EOFs (Fig. 3) shows short-term variations.

Autocorrelation patterns for EOFs 1 and 2 and their cross correlation (Fig. 8) show quite good coherency between them. A perfectly regular oscillation would have a cross correlation oscillating between $\pm 1$ as it would be predictable. The cross correlation in Fig. 8 indicates that the QBO is a regular feature but not perfectly periodic. The cross correlation of 75% after a QBO period explains about 50% of the variance of the next QBO cycle. The cross correlation of the first two EOFs in the standard analysis is 60% after one period. The introduction of time delay into the analysis thus gives a more predictable signal.

In summary, the dominant QBO signal in the zonal-mean zonal wind is a clean oscillation with a well-defined peak near 28 months. It has a fairly regular structure but is not perfectly linear.

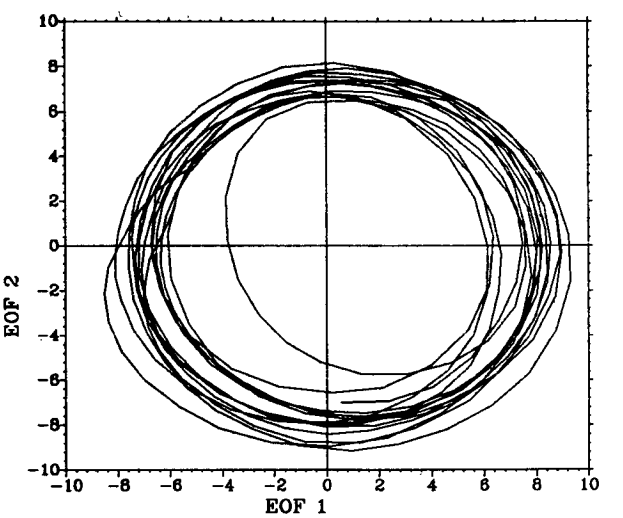


FIG. 7. The phase portrait of EOFs 1 and 2, that is, $A_1$ versus $A_2$.

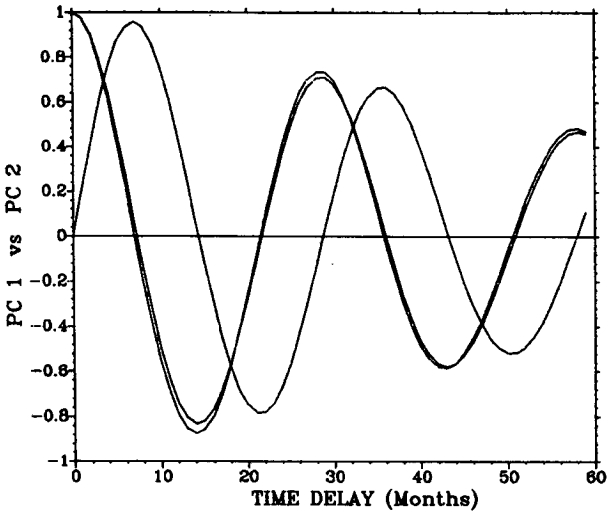


FIG. 8. Autocorrelations of EOFs 1 and 2 and their cross correlation.

The reconstruction of the QBO from these two EOFs (Fig. 5b) showed that the gross structure of the oscillation could be well represented when both phases progress smoothly downwards. Between January 1980 and April 1991 the onset of the easterly phase of the QBO was delayed between 30 and 50 hPa on each occasion (Fig. 9a). The absence of the delay from the reconstruction of the QBO from EOFs 1 and 2 (Fig. 9b) indicates that the signal of the delayed onset is contained in EOFs of higher order.

### 3) DELAYS IN THE ONSET OF WESTERLY WINDS

Inclusion of further EOFs into the reconstructed time series brings it closer to reality by introduction of the delay in the onset of easterly winds. This occurs first with EOF 3, but EOFs 4 and 5 are also needed to yield a realistic structure. The reconstruction with EOFs 1–5 (Fig. 9c) shows that these three EOFs account for the dominant structure of the delayed onset. Inclusion of more EOFs in the reconstruction introduces more detail into the QBO but leads to no better understanding of the dynamics involved.

The height–time delay structures of EOFs 3–5 and their amplitudes (Fig. 10) show that these are not perfectly propagating waves, as in the case of the first pair of EOFs. EOF 3 shows a positive anomaly at high levels at delayed times of more than 6 months but negative anomalies elsewhere; it represents an increase in vertical shear of the wind (when $A_3 > 0$). A recombination of the QBO with EOFs 1–3 leads to the appearance of delays in the onset of easterlies. EOFs 4 and 5 have a more wavelike characteristic, but they do not represent a perfectly propagating wavelike motion like EOFs 1 and 2, as can be seen in the differences in their structure and the irregularities in their amplitudes.

These three EOFs have quite white spectra, with long (several year) and short (sub-QBO time scale) variations. There is apparently no annual cycle in their variability: plots of their amplitude as a function of month show no peaks. There is some evidence of semiannual variability in EOFs 4 and 5. EOF 3 is apparently modulated by EOFs 1 and 2, consistent with it representing

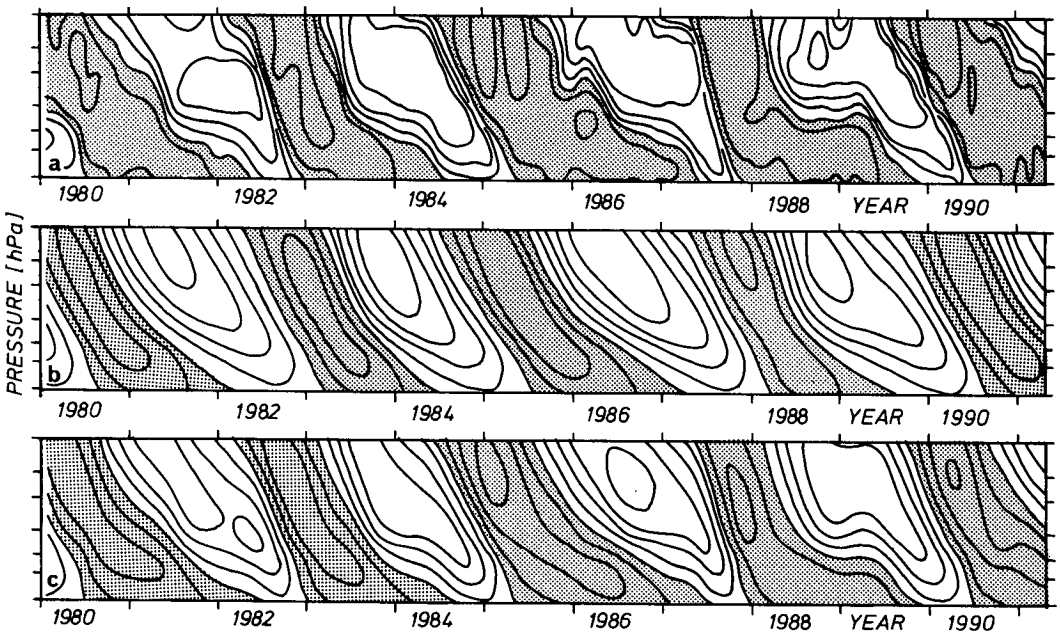


FIG. 9. (a) Time series of zonal wind data from January 1980 to April 1991. (b) Reconstruction of this time series using EOFs 1 and 2 with $W = 15$; (c) Reconstruction of this time series using EOFs 1–5 with $W = 15$. The lightly shaded regions represent easterly winds.

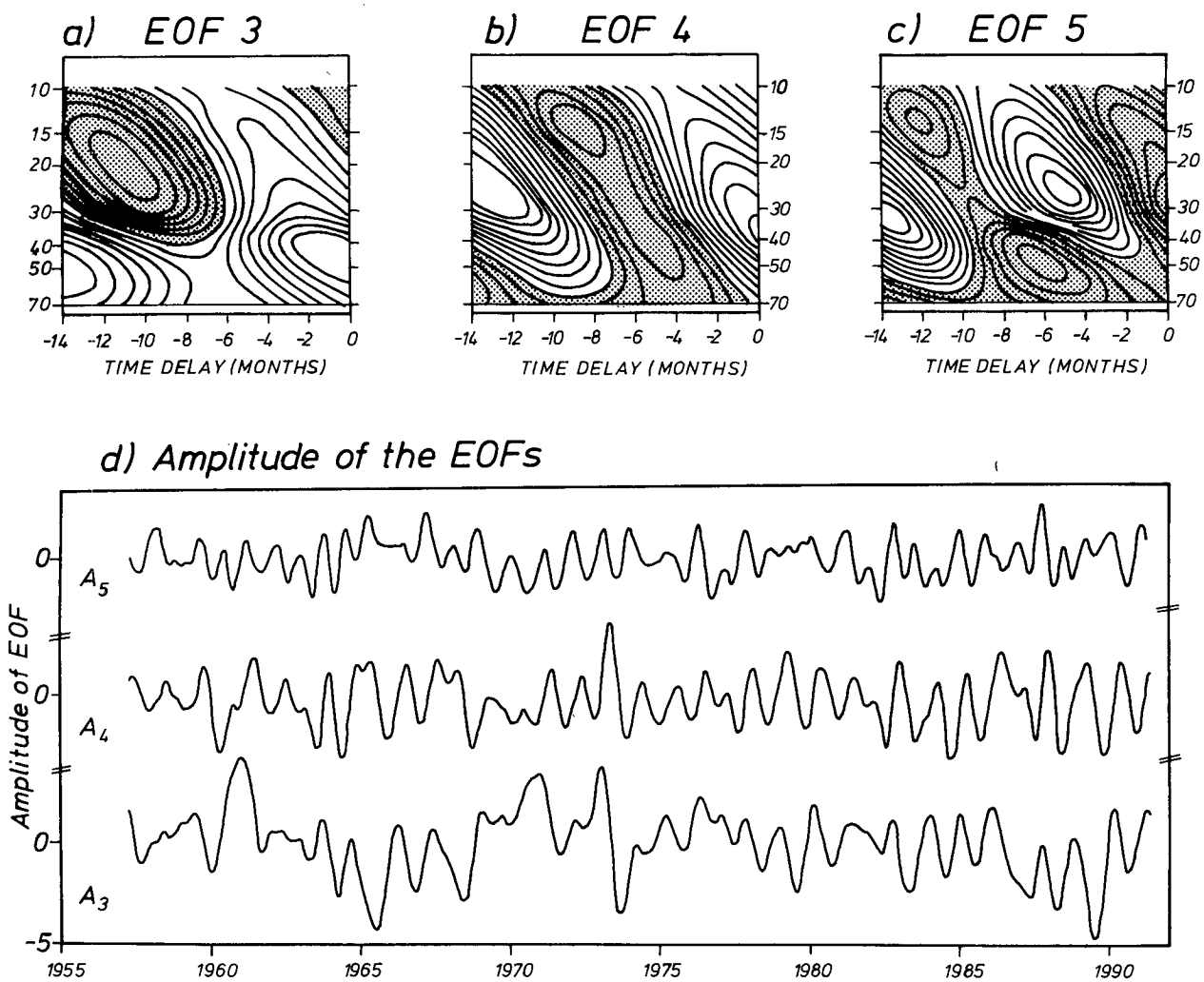


FIG. 10. (a)–(c) EOFs 3–5 with $W = 15$ (lightly shaded areas are negative and the contours are arbitrary). (d) Time series of $A_3$, $A_4$, and $A_5$.

the delay in onset of the easterly phase of the QBO; peaks in $A_3$ tend to occur at extreme values of $A_2$ and minima of $A_1$.

The nonlinearity of these features is evident in their cross and autocorrelations, which show a rapid decrease within one year and remain small before increasing again after another 2–3 years.

#### 4) FURTHER COMMENTS—TRENDS

EOFs of even higher order, representing 3%–1% of the total variance of the time series will not be discussed in great detail here, but we note that some influences from solar and volcanic activity may be included in them. These show up better with $W = 40$, as is expected because of the smoothing of shorter-period oscillations with this window. The "solar signal," included in EOF 5 with $W = 40$ (which is similar to EOF 3 with $W = 15$), shows an increase in vertical wind shear in solar minimum and a decrease in solar maximum; however, this is only apparent over two of the three solar cycles in the wind data. The "volcanic signal" (EOF 12 with $W = 40$) peaks in 1963 and 1986, shortly after the eruptions of Mt. Agung and El Chichón. These are nonpropagating signals in the analysis. They are not statistically significant due to the length of the signal in comparison to the sample size.

## 5. Conclusions and discussion

Using an EOF analysis of the vertical–time delay structure of the zonal-mean zonal wind data from Singapore, the dominant dynamical features of the QBO have been isolated. The first two EOFs represent a regular, downward-propagating oscillation with a dominant period near 28 months, which corresponds well with the known QBO (e.g., Naujokat 1986). The QBO in the vertical–time delay analysis is much more distinctive than that obtained by an EOF analysis of the spatial structure of the wind data, being a much cleaner oscillation with a well-defined period, amplitude, and wavelike structure. This illustrates the power of the

analysis technique in isolating the evolution of quasi-regular oscillations such as the QBO.

The regularity of the dominant QBO in this analysis lends support to the HL model of the QBO at the equator, at least to the extent that the oscillation is forced by some quasi-steady mechanism. The steady descent of the westerly wind regimes and the change in descent rate of the easterlies near 50 hPa is not readily interpreted in terms of the HL model, but some generalization to two dimensions could account for this; alternatively, it could be that the delay in onset is sufficiently strong to influence the dominant structure of the mean wind evolution.

The identification of the delay mechanism as a nonlinear, nonpredictable dynamical feature suggests that it may be due to some form of "external" modulation from the extratropics. A referee has criticized our interpretation of EOFs 3–5, since the results of North et al. (1982) suggest that eigenvectors may be degenerate when the eigenvalues of a noisy dataset are not well separated. We note that the recent results of an EOF analysis of a combined dataset of the tropical winds and 50-hPa Northern Hemisphere geostrophic winds include identical patterns in the tropics with an extratropical component. This suggests that the degeneracy may not be a problem and lends support to our hypothesis that the extratropical dynamics may be responsible for the delay in onset of the westerly phase of the QBO (Pawson et al., 1993). Possible mechanisms are planetary waves propagating equatorward from the winter hemisphere or some manifestation of the residual circulation. This will be the subject of future studies using more spatial dimensions in the EOF analysis and numerical models. In contrast to the results of Dunkerton (1990), our results show no annual dependence; the nonlinear features are, however, related to the dominant QBO in the first two EOFs.

The introduction of the time delay technique into the EOF analysis has been proven to be successful in the isolation of propagating features in the time series of spatial data. The method is generally applicable in three-dimensional space and will be used in future studies of the propagation of disturbances in the atmosphere. Application of EOF analysis with time delay coordinates to the QBO has shown how the propagating part of the signal can be extracted from the noisy dataset where conventional EOFs do not always progress. Furthermore, this method serves as a natural, scale-related filter, treating simultaneously the temporal development of spatial patterns and not artificially separating them.

*Acknowledgments.* We are grateful to Mrs. B. Naujokat for proving the data used in this study. Mrs. B. Mitschke provided invaluable assistance with the figures. The research was supported by the Free University of Berlin and the BMFT, Grant 07KFT306. A referee drew our attention to the results of Weare and Nasstrom (1982) and Rasmusson et al. (1990).

## REFERENCES

Andrews, D. G., and M. E. McIntyre, 1976: Planetary waves in horizontal and vertical shear: The generalized Eliassen–Palm relation and the mean zonal acceleration. *J. Atmos. Sci.*, **33,** 2031–2048.

Broomhead, D. S., and G. P. King, 1986: Extracting qualitative dynamics from experimental data. *Phys. D,* **20,** 217–236.

Dunkerton, T. J., 1985: A two-dimensional model of the quasi-biennial oscillation. *J. Atmos. Sci.*, **42,** 1151–1160.

——, 1990: Annual variation of deseasonalized mean flow acceleration in the equatorial lower stratosphere. *J. Meteor. Soc. Japan,* **68,** 499–508.

——, and D. P. Delisi, 1985: Climatology of the equatorial lower stratosphere. *J. Atmos. Sci.*, **42,** 376–396.

Fraedrich, K., 1986: Estimating the dimensions of weather and climate attractors. *J. Atmos. Sci.*, **43,** 419–432.

——, and M. Lutz, 1987: A modified time–longitude diagram applied to 500 mb heights along 50° north and south. *Tellus,* **39A,** 25–32.

Hamilton, K., 1984: Mean wind evolution through the quasi-biennial cycle in the tropical lower stratosphere. *J. Atmos. Sci.*, **41,** 2113–2125.

Holton, J. R., and R. S. Lindzen, 1972: An updated theory for the quasi-biennial oscillation of the tropical stratosphere. *J. Atmos. Sci.*, **29,** 1076–1080.

Lindzen, R. S., 1971: Equatorial planetary waves in shear: Part 1. *J. Atmos. Sci.*, **28,** 609–622.

——, and J. R. Holton, 1968: A theory of the quasi-biennial oscillation. *J. Atmos. Sci.*, **25,** 1095–1107.

Maruyama, T., 1991: Annual and QBO-synchronized variations of lower-stratospheric equatorial wave activity over Singapore during 1961–1989. *J. Meteor. Soc. Japan,* **69,** 219–232.

Naujokat, B., 1986: An update of the observed quasi-biennial oscillation of the stratospheric winds over the tropics. *J. Atmos. Sci.*, **43,** 1873–1877.

——, K. Labitzke, R. Lenschow, K. Petzoldt, B. Rajewski, and R.-C. Wohlfart, 1991: The stratospheric winter 1990–91: A major midwinter warming as expected. *Beilage zur Berliner Wetterkarte.*

North, G. R., T. L. Bell, R. F. Cahalan, and F. J. Moeng, 1982: Sampling errors in the estimation of empirical orthogonal functions. *Mon. Wea. Rev.*, **110,** 699–706.

Pawson, S., K. Labitzke, B. Naujokat, R. Wang, and K. Fraedrich, 1993: Intraseasonal tropical–extratropical interactions observed in the stratosphere. *Coupling Processes in the Lower and Middle Atmosphere.* E. Thrane, T. Blix, and D. Fritts, Eds., Kluwer, 35–47.

Plumb, R. A., and R. C. Bell, 1982: A model of the quasibiennial oscillation on an equatorial beta plane. *Quart. J. Roy. Meteor. Soc.*, **108,** 335–352.

Rasmusson, E. M., X. Wang, and C. F. Ropelewski, 1990: The biennial component of ENSO variability. *J. Mar. Sys.*, **1,** 71–96.

Reed, R. J., W. J. Campbell, L. A. Rasmusson, and D. G. Rogers, 1961: Evidence of the downward-propagating annual wind reversal in the equatorial stratosphere. *J. Geophys. Res.*, **66,** 813–818.

Veryard, R. G., and R. A. Ebdon, 1961: Fluctuations in tropical stratospheric winds. *Meteor. Mag.*, **90,** 125–143.

Vautard, R. and M. Ghil, 1987: Singular spectrum analysis in nonlinear dynamics with applications to paleoclimatic time series. *Phys. D,* **35,** 395–424.

Wallace, J. M., L. Panetta, and J. Estberg, 1993: Representation of the equatorial stratospheric quasi-biennial oscillation in EOF phase space. *J. Atmos. Sci.*, **50,**1751–1762.

Weare, B. C., and J. S. Nasstrom, 1982: Examples of extended empirical orthogonal function analyses. *Mon. Wea. Rev.*, **110,** 481–485.

Xu, J.-S., 1992: On the relationship between the stratospheric quasi-biennial oscillation and the tropospheric southern oscillation. *J. Atmos. Sci.*, **49,** 725–734.